# Structure and magnetic field of the July 11, 1991 eclipse corona from the solar cycle viewpoint

**J. Sýkora**[1], **O.G. Badalyan**[2], **V.N. Obridko**[2] **and T. Pintér**[3]

[1] *Astronomical Institute of the Slovak Academy of Sciences, SK-059 60 Tatranská Lomnica, The Slovak Republic*

[2] *Institute of Terrestrial Magnetism, Ionosphere and Radio Wave Propagation, 142092 Troitsk, Moscow Region, Russia*

[3] *Slovak Central Observatory, SK-947 01 Hurbanovo, The Slovak Republic*

Received: June 30, 1999

**Abstract.** A set of the white-light images was used to perform relative photometry of the July 11, 1991 eclipse corona. The observed global form of that day corona was found to be rather unusual for the actual solar cycle phase. In this relation, the recently calculated coronal magnetic field structures and strengths are presented and discussed. An idea on the close relation between the observed global form of the corona and the presence of the individual coronal structures around the solar limb, on the one hand, and the calculated magnetic field topology and strength, on the other hand, is supported and found to be of great interest.

**Key words:** solar eclipse corona – photometry – magnetic field – solar cycle connections

## 1. Introduction

For a long time, there have been increasing indications about a close relationship between the solar magnetic field hierarchism and a variety of the observed coronal structures (e.g., Beckers, 1971). The evolution of the global coronal magnetic field during the solar cycles is now also well understood (e.g., Figs. 2-3 in Hoeksema, 1993). The relationship mentioned is due to the MHD effects on the alignments of different coronal structures and the global MF evolution is derived for the commonly accepted coronal source surface at the distance $r = 2.5\,R_{\odot}$ assuming that the field is a potential field, i.e. no significant currents flow in the corona. Typically, near solar cycle minima the global heliomagnetic equator is almost identical to the heliographic equator, while at the cycle maxima the magnetic equator is usually more wavy, highly inclined to the heliographic equator and often reaching the solar poles. The aim of this paper is to demonstrate and discuss the structure/magnetic field resemblance for a special configuration of the 11 July 1991 eclipse corona. In addition, our calculations of the coronal magnetic field strength represent quite a new phenomenon in this analysis.

Sometimes, apparently well-established knowledge needs to be revised in the light of newly observed facts. In our opinion, this is the case with the generally accepted changes of the coronal form in the course of the 11-year solar cycle. In this context it should be emphasized that the most pronounced structures, defining the global form of the corona during the eclipses, are the helmet streamers. They create a more or less continuous belt around the Sun distributed just over the heliomagnetic equator (Bruno et al., 1982; Wilcox and Hundhausen, 1983; Koutchmy and Livshits, 1992). The integration and linkage of the observed July 11, 1991 coronal form into the concept of the global magnetic field structure and topology evolution is treated in the present paper and explains some more of this three-dimensional problem.

## 2. The white-light corona at the eclipse day

The observation was carried out during the 11 July 1991 eclipse (at about $18^h\,50^m$ UT) in Mexico, Baja California, La Paz ($\lambda = -110°$ 15' 27", $\phi = +24°$ 09' 24", h = 10 m) under very good weather conditions. Three images of the white-light corona (1/60, 1/15, and 1/4 second exposures), taken with an 10/100 cm telescope, were subjected to detailed photometric and computer processing. A space resolution of about 10 arcsec was achieved. Finally, the three images were combined to obtain the isophotes of the $K + F$ corona in the broader range of distances from the disk centre.

The sketch of the coronal structures shown in Fig. 1 was drawn using the well-known technique of overlapping the photographic negative and positive with a mutual angular displacement of them for a very small angle. Although the epoch was relatively soon after the recent solar maximum, the global flattening of the corona, surprisingly, resembles that expected during the epochs close to the minimum of the solar cycle. However, there is one substantial difference: the huge coronal streamers, decisively determining the global form and flattening of the corona, are now recorded at very high solar latitudes and not close to the equator as is typical for the periods of the solar cycle minima. In the Section 4 this peculiarity is demonstrated as a direct consequence of the specific position and orientation of the heliomagnetic equator (a neutral sheet) which separates the northern and southern magnetic polarities on the source surface $r = 2.5\,R_{\odot}$. It is also underlined why in the past the corona was believed to be always nearly spherical in the periods of the solar cycle maxima.

Conventionally, we refer throughout this paper to the heliographic position angles $P$ measured counterclockwise from the heliographic north pole (indicated, for example in Fig. 1). A considerable variety of the coronal features, not commonly observed at the solar cycle maxima, were seen around the limb at

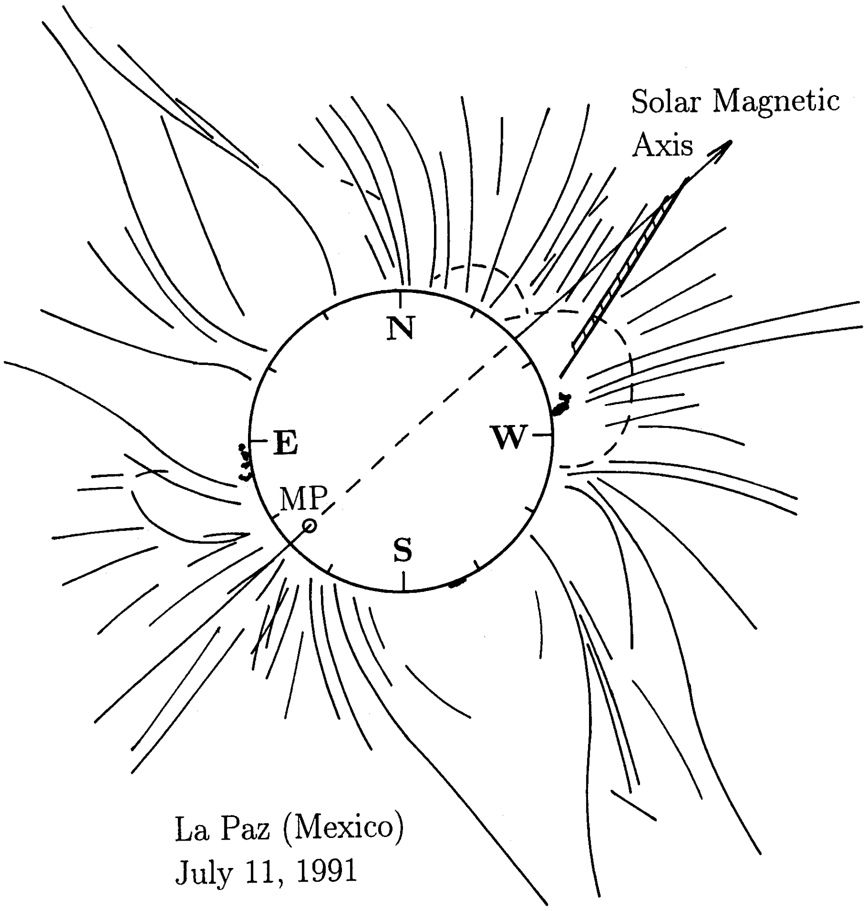


**Figure 1.** The sketch of the coronal structures as drawn from the July 11, 1991 eclipse images.

the eclipse day. The most remarkable of the structures are:
– The expressive radially aligned helmet streamer (from position angle 20° to 60°), with an indication of some other structure behind the scene.
– A somewhat less pronounced and more structured streamer appears close to the east equator ($P = 65° - 105°$) with a prominence at the typical position "under the streamer's dome". This streamer is highly nonradial.
– The region to the south – up to $P = 135°$ is relatively complicated in its structure and bearing signs of activity present in the middle solar latitudes.
– Then, at $P = 135° - 160°$, a coronal hole-like structure is observed. Our computer-processed image (not published here) indicates a number of polar rays within it.

– Over the south pole and further to the west limb ($P = 160° - 265°$) the huge system of about 3–4 streamers is found in superposition. Again, under the largest streamer, a small prominence is recorded at $P = 200°$. Similarly to the filaments visible on the solar surface in $H_\alpha$, the prominences under the streamers undoubtedly indicate the presence of the neutral magnetic line.
– Advancing to the west equator, more tiny structures appear (up to $P = 315°$), reflecting activity in the photosphere. Some of the active rays (for example, those starting from the prominence at $P = 280°$) are highly nonradial.
– At the same time, most of the NW-quadrant (up to $P = 345°$) is also occupied by two "mound" structures, the southern being much brighter and larger than the northern one.
– A number of polar rays are detected over the north pole ($P = 320° - 10°$), partially overlapping the weaker northward "mound". The indicated region bears all the typical indications of the polar coronal hole (see also the analysis of the white-light and green-line polarization measurements performed in Badalyan, Livshits and Sýkora, 1997; Badalyan and Sýkora, 1997).
– It can be summarized that the overall configuration of the white-light corona observed is, in principle, determined by the presence and the actual distribution of the streamers and coronal holes around the solar limb at the eclipse day. Both these phenomena are believed to be of MHD origin. In our case the global form of the corona evokes a magnetically dipolar structure, with a streamer belt over the highly inclined heliomagnetic equator and with two coronal holes over the heliomagnetic poles, which are remarkably displaced from the heliographic poles. Moreover, the flattened appearance of the July 11, 1991 corona suggest a configuration typical of times other than close to the maximum of the solar activity cycle. An explanation of the found peculiarities in the global form of the corona is attempted below.

A more quantitative approach to the outlined findings is not necessarily advantageous. For example, our detailed photometry provided the isophotes in Fig. 2. The comparison with Fig. 1 shows that the intensity plot is not very effective in identifying the individual large-scale coronal structures. In this sense, the measurement of the white-light corona polarization is more productive, especially in combination with the intensity measurements (Badalyan, Livshits and Sýkora, 1997). In so doing, the physical parameters of the streamers and coronal holes can also be estimated and discussed.

The isophotes in Fig. 2 (drawn in step $\Delta \log I = 0.2$) indicate the highest brightness at the low latitudes, reflecting activity in the vicinity of the solar equator. On the other hand, the isophotes are clearly elongated in the direction where the huge streamers are present at the high solar latitudes. These facts represent a serious inconsistency. When measuring the solar corona flattening according to the well-known and generally accepted Ludendorff's definition (Ludendorff, 1928), a value very close to $\varepsilon = 0.00$ is obtained. Expressed in words, the 11 July 1991 corona should be perfectly circular in form. Such a value would be very acceptable from the aspect of the actual near-maximum phase of the

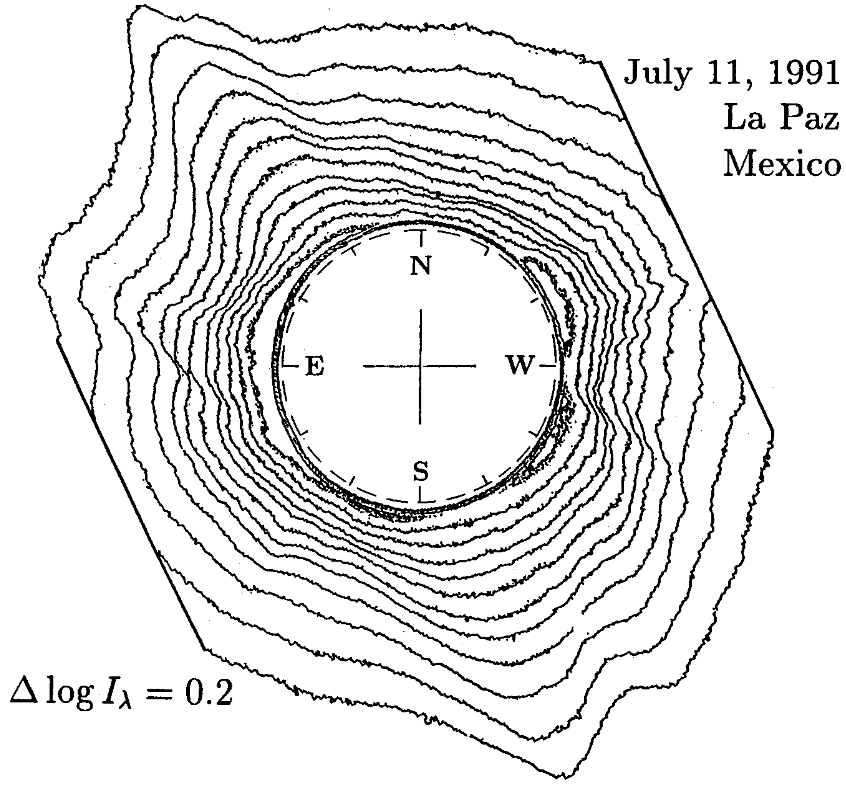


**Figure 2.** The isophotes of the white-light corona.

22nd solar cycle (for the definition of the solar cycle phase see Mitchell, 1929) but, unfortunately, it is in severe disagreement with the actual observed coronal form. In fact, the 1991 corona is found considerably flattened. However, the flattening is not towards the heliographic equator but towards the heliomagnetic equator (see below, and Fig. 3).

## 3. Method of calculation of the magnetic field

One of the ways in which the magnetic field in the solar corona can be inferred is based on the extrapolation of the measured photospheric magnetic field. Our calculations of the coronal magnetic field were performed using a well-known method, earlier described by Hoeksema and Scherrer (1986). This method assumes that the magnetic field energy in the layers between the photospheric surface and a certain level in the solar corona is higher than the energy of the possible electric currents. In other words, the deviations of the magnetic field structure from a potential character of the field are assumed to be small and, so we ignore them. However, starting from a certain height, the flows of the solar wind plasma are not negligible, the field cannot be considered current-free and the field lines of force are gradually stretched to a practically radial direction. The surface where the lines of force are supposed to be strictly radial and the potential of the field becomes equal zero is called the source surface. Below the source surface the field decreases, on average, by $r^{-3}$, and above this surface (in the interplanetary space) by only $r^{-2}$. This makes it possible to choose the optimum radius of source surface, so that the calculated values of the magnetic field in the interplanetary space near to the Earth will be in agreement with the measured values. In Hoeksema and Scherrer (1986) this radius was taken as 2.5 $R_\odot$, and the same value was utilized throughout all our calculations. We have also used the method of polar correction (Hoeksema and Scherrer, 1986), which is necessary to be applied, because the magnetic fields are measured with the larger errors close to the poles.

Thus, measuring the longitudinal component of the magnetic field at the photospheric level, considering the zero potential at the source surface and assuming the potential approximation of the field inside this spherical layer, we come to the boundary condition problem. Assuming that the field at the lower boundary fulfils also condition of the potential approximation, the solution of our problem can be expressed by the following equations:

$$\begin{aligned} B_r &= \sum P_n^m(\cos\theta)(g_{nm}\cos m\varphi + h_{nm}\sin m\varphi) \times \\ &\quad \left\{(n+1)(R_\odot/R)^{n+2} - n(R/R_s)^{n-1}c_n\right\}, \end{aligned} \tag{1}$$

$$\begin{aligned} B_\theta &= -\sum \frac{\partial P_n^m(\cos\theta)}{\partial\theta}(g_{nm}\cos m\varphi + h_{nm}\sin m\varphi) \times \\ &\quad \left\{(R_\odot/R)^{n+2} + (R/R_s)^{n-1}c_n\right\}, \end{aligned} \tag{2}$$

$$\begin{aligned} B_\varphi &= -\sum \frac{m}{\sin\theta}P_n^m(\cos\theta)(h_{nm}\cos m\varphi - g_{nm}\sin m\varphi) \times \\ &\quad \left\{(R_\odot/R)^{n+2} + (R/R_s)^{n-1}c_n\right\}. \end{aligned} \tag{3}$$

Here, $0 \le m \le n \le N$ (usually, $N = 9$), $c_n = -(R_\odot/R_s)^{n+2}$, $P_n^m$ are the Legendre polynomials, $g_{nm}$ and $h_{nm}$ are the coefficients of the spherical harmonic analysis based on the original magnetic data, $\theta$ represents the solar latitude counted from the north pole, $\varphi$ is the Carrington longitude and $R_s$ is the source surface radius (all the distances are expressed in terms of the solar radius).

The magnetic fields regularly measured at the John Wilcox Observatory (Stanford University) was used as the basic data. This data is presented in the form of longitudinal magnetic field synoptic charts, prepared for the succession of Carrington rotations. The measurements are realized with a resolution of 3 arc minutes. The charts are prepared in table form, with an interval of five longitudinal degrees and with 30 points in the sine of latitude from the north to the south pole. At the same time, there is no data from latitudes higher than 70°.

In this work, software allowing us to calculate the synoptic charts of the magnetic field strength distribution at any given height for any moment (to be more exact, for a date corresponding to the central meridian of the chart) was also used. The full vector of the magnetic field strength is considered here and after. The data obtained is in the form of a network with dimensions of 80 points in the solar longitude and 100 points in the latitude. The calculations over the latitude are performed for the interval $\pm 70°$ only. Thus, each synoptic chart is obtained with the resolution 4.5° in the longitude and 1.4° in the latitude. The data for the east and west limbs can be found at the longitudes $\pm 90°$ from the central meridian. The charts were constructed for all the distances from $1.0\,R_\odot$ to $2.5\,R_\odot$ with a step $0.05\,R_\odot$. Then, for each point of the network, related to the E and W limbs, the altitude course of the magnetic field strength was possible to obtain. Subsequently, for each of the network points the distance from the solar disc centre was found at which the magnetic field strength reaches a given value (in our case, for example, 40, 60, 100, 150 and 200 $\mu T$ in Fig. 4).

One should notice that the procedure of the magnetic field calculations still has a number of shorcomings. Nowadays, it is known that the field above the photosphere is not quite current-free. At the photospheric level and above the photosphere noticeable currents and major plasma motions are observed. Nevertheless, these currents and flows are mostly connected with relatively small-scale structures. It is also not realistic to assume a jump-like transition from the potential field to the solar wind field. However, it is easy to demonstrate that the influence of the source surface is determined by the second term in the curly braces of the Eqs. (1)-(3), and that for the calculations close to the photosphere this contribution is quite small. Therefore, our approximation is hopefully reasonable, when sufficiently large-scale and steady-state structures are investigated. In addition, applying the described procedure, a certain inaccuracy can arise due to the inclination of the solar rotation axis (reaching $\approx 4°$ in July) and, also some differences in the averaged observed values of the magnetic field at different latitudes may appear. The calculations would be much more complicated when taking into consideration both these effects, while the final results would be only slightly different.

## 4. Comparison of the calculated magnetic field with the structures and global form of the July 11, 1991 corona

The upper part of Fig. 3 shows the structure of the magnetic field lines of force as calculated for the July 11, 1991 corona. The left panel demonstrates the open and closed field lines of force, rising from the regular network at the basement of the corona. A certain part of the lines of force is closed back to the photosphere while, another part of them rises up to $2.5\,R_\odot$ and goes out into the interplanetary space. The chart of the radial field $B_r$ (as calculated for the photospheric level) is plotted in this left panel, where the full lines indicate the N-polarity and the S-polarity is drawn using dotted lines. Because, in this case, a regular network on the photospheric surface was utilized to obtain the structures, and only a relatively small part of the photosphere is occupied by regions with open lines of force, the upper left panel of Fig. 3 mostly shows the structures with the closed field lines of force.

The open lines of force structures are better illustrated within the upper right panel of Fig. 3. In this case, we have utilized a regular network on the source surface, where, according to definition, the magnetic field lines of force become open. Each of the lines of force is traced down to the photospheric surface. Again, the $B_r$ chart is plotted, as calculated for the source surface and projected onto the normal surface ($r = 1.0\,R_\odot$). The neutral line should be noticed, demonstrating the particular position of the highly inclined heliomagnetic equator close to the central meridian and indicating the basement of the heliospheric current sheet. As mentioned above, particularly over this line the coronal streamers are distributed all around the Sun.

The comparison of the upper part of Fig. 3 with the actual observed structures of the July 11, 1991 corona (Fig. 1) shows that, apart from all the simplifications used during the process of calculations, the derived magnetic structures correspond well enough to the type and distribution of the observed coronal structures. The closed magnetic structures are distributed over the heliomagnetic equator and agree well with the positions of the streamers. The magnetically open regions are dominant above the poles of the calculated global magnetic field. It is evident that the heliomagnetic equator, localized close to the central meridian, was viewed edgewise from the Earth on the eclipse day (Gulyaev, 1992a, 1992b; Saito et al, 1993; Sýkora and Ambrož, 1995). The global form of the corona was found evidently flattened towards this equator.

The distribution of the magnetic field strength around the disk and in dependence on the distance from the disk centre is shown in Fig. 4 (this figure was obtained by the procedure described in the third section of this paper). Apart from the relatively rough calculations, it is possible to state that the magnetic fields of the bright equatorial condensations differ by as much as three times the field strengths found in the high latitude streamers of the July 11, 1991 corona, being at the distance $1.2\,R_\odot$ about 150 $\mu T$ and 50 $\mu T$, respectively. From the nature of the calculations, it follows that these values are, of course,

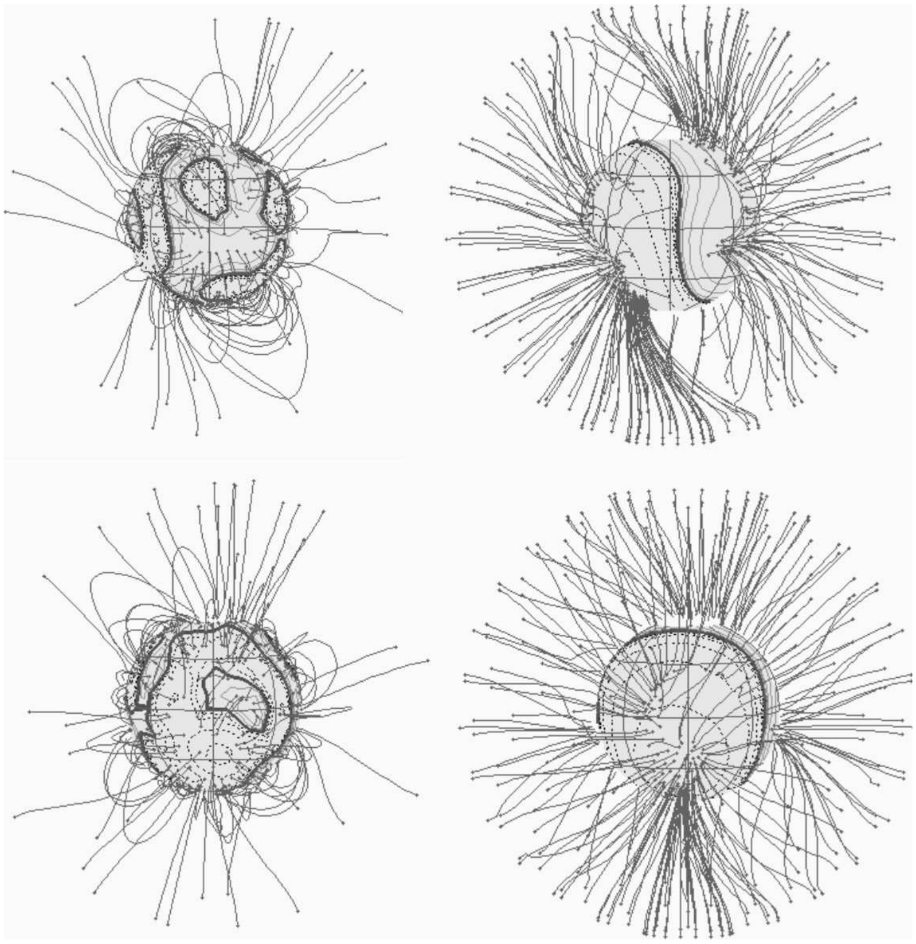

**Figure 3.** The calculated closed (on the left side) and open (on the right side) magnetic field lines of force for 11 July 1991 (upper panels) and 15 July 1991 (lower panels). The solar north is above and the east is to the left. See more details in the text.

averaged over a certain area. The magnetic field strengths inside the particular small-scale flux tubes may be much higher.

In Fig. 4, the isolines of the magnetic field strength in the corona i.e. the "isogausses", are presented. (The term "isogausses" for the lines of the equal magnetic field strength is used. This term is in no way related to the physical unit $\mu T$ in which the field strengths are expressed.) As far as we know, this kind of coronal magnetic field presentation has not been produced earlier. The comparison of the isogausses with the structure of the isophotes (Figs. 2 and 4) reveals an evident difference in their behaviour. The isogausses are stretched in the direction of the magnetic poles and compressed at the magnetic equator.

This means that the isogausses and the isophotes form two systems of mutually orthogonal curves. Such a feature is demonstrated for the first time and seems to be very promising scientifically.

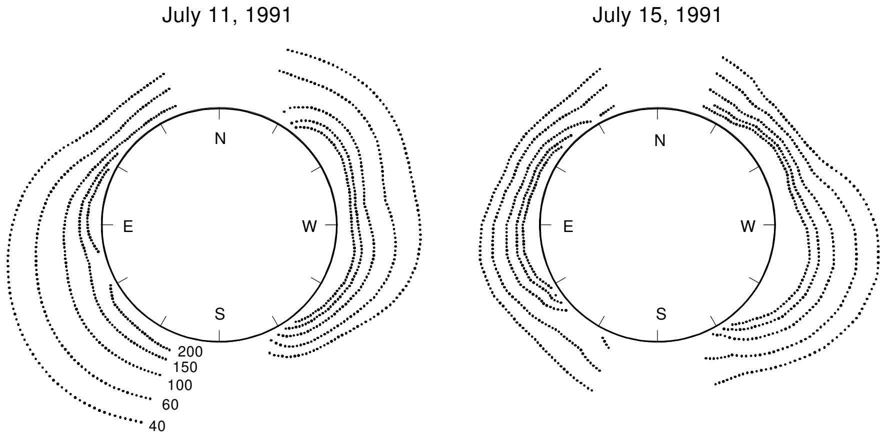


**Figure 4.** The charts of the magnetic field strengths as derived for the eclipse day and four days later. The isogausses are 200, 150, 100, 60 and 40 $\mu T$ preceeding from the solar limb.

The mentioned orthogonality represents a direct consequence of the basic statement that the solar corona is a flat phenomenon (feature). In such a corona the magnetic field is preferentially described by a dipole configuration. As it is known, the magnetic field is about two times higher at the dipole poles in comparison with that at the equator, at the same distance from the solar disk centre. That is why, the isogausses create a system of the closed oval-type curves, with the large axis directed along the dipole axis. At the same time, the huge streamers are distributed in the zone around the dipole equator, causing a pulling-out of the isolines of equal brightness (the isophotes) in the direction perpendicular to the axis of the magnetic dipole. Naturally, the orthogonality is best visible at the larger distances from the disk centre.

The described picture is the most distinctly visible when the dipole with the axis identical with the solar rotation axis is observed. Then, the orthogonality effect is visible at any angular turn of the Sun (the solar corona at the minima of the solar activity cycles). In case of the inclined dipole, such a picture is observed when the observer is situated very near to the plane of the heliomagnetic equator. After seven days, when the Sun rotates and the observer is found in the plane perpendicular to the plane of the heliomagnetic equator, the orthogonality effect is lost, because like the isolines of the magnetic field strength, the isolines of brightness become strictly circular. Therefore, the considered orthogonality effect can be detected in the phase near to the solar cycle minimum, or near to the maximum of solar activity, due to the specific position of the observer, as was the case in the July 11, 1991 solar eclipse.

The conclusion about a double role of the magnetic field in forming the solar corona can be pronounced. Firstly, under the influence of the magnetic field the coronal structures, differing by the physical conditions inside them (mainly the plasma density), are created. The stronger and more complex magnetic fields in the near-equatorial regions lead to the appearance of the more active and dense coronal loops and condensations in these parts of the solar surface and, at the same time, the more rarefied and magnetically more simple coronal streamers are characterized by the lower magnetic field strengths. Secondly, the observed global form of the corona is pre-determined by the inclination of the heliomagnetic equator relative to the heliographic equator and, at these times, by its position with respect to the central meridian of the Sun (i.e., with respect to the line of sight). Then, the observed apparent global form of the corona is given by the actual plane-of-sky projection of the coronal streamers encircling the heliomagnetic equator. During the July 11, 1991 eclipse the magnetic equator was evidently edgewise viewed and the corona was clearly flattened towards it.

## 5. How the global form of the corona changes due to solar rotation

Briefly after the 1991 eclipse we tried to understand the unusually flat form of the corona observed. In this connection the Ludendorff's definition of the coronal flattening was criticized as defective and misleading (Sýkora and Badalyan, 1992). A number of papers appeared (Gulyaev and Vanyarkha, 1992; Gulyaev 1992a, 1992b; Saito et al., 1993) pointing out the role of the three-dimensional geometry in viewing the coronal disk formed by the streamer belt over the heliomagnetic equator. Referring to the regularities found in the long-term evolution of the coronal magnetic field at the source surface (see, e.g., Figs. 2-3 in Hoeksema, 1993) a confrontation of three minimum-like eclipse coronae occurring in 1994, 1995 and 1997 and two near-maximum coronae (taking place in 1980 and 1991) with the calculated magnetic field topologies was performed (Sýkora and Ambrož, 1995, 1997; Sýkora et al., 1998). The important role of the actual position of the heliomagnetic equator in relation to the solar central meridian for the observed form of a given corona (which always represents a plane-of-sky projection of the real three-dimensional corona), was identified. The coronal form is understandably flat when the heliomagnetic equator is more or less identical with the heliographic equator during the solar cycle minimum but, it also remains surprisingly flat in the period of the solar cycle maximum if the heliomagnetic equator is localized close to the central meridian of the Sun, i.e., this equator is edgewise viewed from the Earth. This was exactly the case in the 11 July 1991 eclipse.

The calculated magnetic field, shown in the lower part of Fig. 3, demonstrates the probable form of the corona if the eclipse had taken place on 15 July 1991. It is evident that after only four days the form of the corona would be completely different. The closed structures (left panel) would be visible all around the disk, correspondingly to the position of the neutral magnetic line close to the limb (see the right panel with the circularly symmetrical open structures). Apparently, due to plane-of-sky projection of the streamer belt, much less rotation of the Sun (about 2-3 days only) would be necessary "to destroy" the significantly flattened 1991 corona. This is why the flattened eclipse corona has been so rarely observed in the past during the solar cycle maxima. The influence of the solar rotation is clearly seen in the change of the magnetic field isogausses (the right panel in Fig. 4), where a properly tilted and relatively symmetrical distribution of the isolines is derived for July 15, 1991.

The influence of the solar rotation is quite different on the observed coronal forms in the minimum periods of the solar cycles. In these periods the neutral magnetic line (the heliomagnetic equator) is approximately identical to the plane of the heliographic equator and, consequently, the observed coronal form is not significantly disturbed by the solar rotation. Therefore, during several successive solar rotations the form of the corona may change negligibly (Sýkora et al., 1998; Koomen et al., 1998).

## 6. Variations of the coronal form as a function of phase in the solar cycle

The shape (form) of the solar corona has long been determined by the Ludendorff flattening coefficient. It is defined as:

$$\varepsilon = \frac{d_e}{d_p} - 1, \tag{4}$$

where $d_e$ and $d_p$ are the equatorial and polar distances of the same isophote, and obtained as the means of the values at three positions: $0°$, $\pm 22.5°$ and $90°$, $90° \pm 22.5°$, respectively. It is recommended the isophote at $0°$ is chosen at the distance about $2.0\,R_\odot$. All the previous textbooks and a large number of the past papers declared, without any reservations, a clear sine curve dependence of the flattening index on the phase in the solar cycle. The flattening was believed to be small ($\approx 0.05$) during the solar maxima (*maximum circular corona*) and large ($\approx 0.25$) during the solar minima (*minimum flattened corona*).

Recognizing the long-term evolution of the global magnetic field topology on the source surface, considering a clear morphological and the physical affiliation of the coronal streamers to the evolutionary tilting heliomagnetic equator, and bearing in mind the indisputable dependence of the observed apparent coronal form on the solar rotation and on the two-dimensional plane-of-sky projection, we are now very sceptical about the generally accepted scenario of the coronal form changes during the solar cycle. The doubts were further strengthened by the case of the 11 July 1991 eclipse, when the clear inadequacy of Ludendorff's definition of the coronal flattening was revealed. The derived flattening ($\varepsilon = -0.02$) indicates a perfectly circular corona while, in fact, the corona was observed considerably flattened.

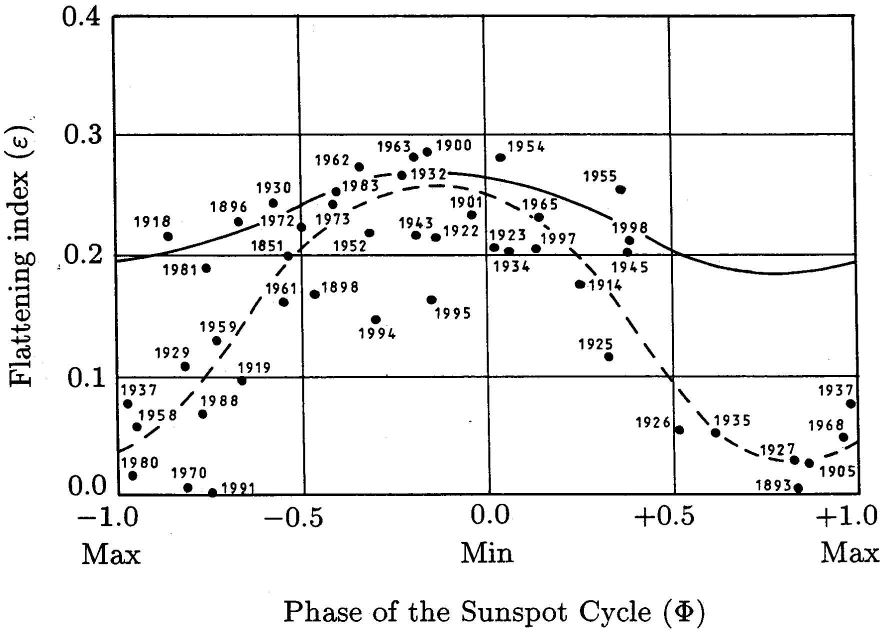


**Figure 5.** Variations in the Ludendorff flattening coefficient as a function of phase in the solar cycle (observed – dashed line, hypothetical and physically reasoned – full line).

Taking into account all the above facts and findings, a hypothesis can be considered that the solar corona is, very probably, always remarkably flattened. However, this flattening is towards the heliomagnetic equator and not towards the heliographic equator. An apparently circular corona, characteristic of the periods of the solar cycle maxima, does not seem to be substantiated physically and can be easily explained by the geometry of the streamers' and their two-dimensional projection onto the plane of the sky. The real three-dimensional form of any individual form of the solar corona undoubtedly corresponds to the actual orientation of the global solar magnetic equator during its long-term evolution over the solar cycle (Hoeksema, 1993). Thus, one can feel that the published (e.g., in the monographs by Kuiper, 1953 and Golub and Pasachoff, 1997) and generally accepted sine curve of the coronal flattening cycle variations is to a large extent fictitious and does not reflect the three-dimensional reality.

The hypothetical full curve sketched in Fig. 5 may represent the physically substantiated variations of the coronal flattening much better.

## 7. Conclusions

- The July 11, 1991 white-light corona displayed a specific global form, unexpected in the near-maximum solar cycle phase. A variety of structures were detected, including the huge streamers at the high solar latitudes and, surprisingly, also coronal holes.
- As usual, isophotes of the coronal brightness are not as effective in identifying the individual coronal structures as photographically or computer processed images are. On the other hand, only the isophotes may provide an important quantity – the coronal flattening index.
- It was found that Ludendorff's definition of the coronal flattening gives very contradictory result for the July 11, 1991 corona. The derived value $\varepsilon = -0.02$ indicates a perfectly circular corona while the general appearance of it is evidently flattened, strongly elongated and, at the same time, considerably inclined with respect to the solar equator.
- The structure and topology of the magnetic field lines of force, calculated for the eclipse day, faithfully reflect the actually observed distribution of the streamers and coronal holes. The global form of the corona resembles a magnetic dipole with the streamer belt over the highly inclined heliomagnetic equator and the coronal holes over the heliomagnetic poles. The observed flattening of the corona is exactly towards the derived magnetic equator and supports the MHD origin of the coronal structures and forms.
- The distribution of the magnetic field strength has a somewhat different character, not necessarily reproducing the topology of the magnetic field lines of force distribution. Despite the comparatively rough calculation, it is possible to declare that the magnetic field in the bright near-equatorial coronal condensations and in the high-latitudinal huge streamers of the 11 July 1991 corona differ by as much as three times and at the distance $1.2\,R_\odot$ it is about 150 $\mu T$ and 50 $\mu T$, respectively.
- The isogausses of the magnetic field are compressed at the magnetic equator and extended at the magnetic poles. For the first time, it is demonstrated that both the isogausses and the isophotes form two systems of mutually orthogonal curves.
- We have found that the observed global form of the corona is drastically influenced by the solar rotation, in particular, in the periods close to the solar cycle maxima. In these periods a considerably flattened corona may be observed as well, on the assumption that the heliomagnetic equator is

edgewise viewed, i.e., in the case that this equator is in position close to the central meridian of the Sun. Only about a 2–3 day solar rotation can cause a quasi-circular corona form, resulting from the plane-of sky projection of the angularly displaced belt of the streamers. This is the principal reason why in the periods near to the solar cycle maxima the flattened corona was observed so rarely in the past. Together with some other authors (Gulyaev, 1992b; Koomen et al., 1998) we have pronounced an opinion (Sýkora and Ambrož, 1995; Sýkora et al., 1998) that the LASCO C2 and C3 coronagraphs at SOHO may prove this scenario during the coming maximum of the solar activity cycle.

– In the light of the preceding points the variations of the coronal flattening index as a function of phase in the solar cycle should be re-evaluated. In our opinion, the solar corona is most likely always considerably flattened towards the heliomagnetic equator.

**Acknowledgements.** The authors greatly appreciate the support of the VEGA Grant 02/5007/98 of the Slovak Academy of Sciences and the Grant No. 99-02-18346 of the Russian Foundation for Basic Research.

## References

Badalyan, O.G., Sýkora, J.: 1997, *Astron. Astrophys.* **319**, 664

Badalyan, O.G., Livshits, M.A., Sýkora, J.: 1997, *Solar Phys.* **173**, 67

Beckers, J.M.: 1971, in *Solar Magnetic Fields*, ed.: R. Howard, Reidel, Dordrecht, 3

Bruno, R., Burlaga, L.F., Hundhausen, A.J.: 1982, *J. Geophys. Res.* **87**, 10339

Golub, L., Pasachoff, J.M.: 1997, *The Solar Corona*, Cambridge University Press, Cambridge

Gulyaev, R.A.: 1992a, *Solar Phys.* **142**, 213

Gulyaev, R.A.: 1992b, in *Proc. First SOHO Workshop*, ed.: C. Mattok, ESA **SP-348**, Noordwijk, 133

Gulyaev, R.A., Vanyarkha, N.Ya.: 1992, *Solar Phys.* **140**, 369

Hoeksema, J.T.: 1993, in *Solar Terrestrial Predictions - IV*, ed.: J. Hruska, M.A. Shea, D.F. Smart, G. Heckman, NOAA/ERL, Boulder, 3

Hoeksema, J.T., Scherrer, P.H.: 1986, *The Solar Magnetic Field – 1976 through 1985*, WDCA Report **UAG-94**, NGDC, Boulder

Koomen, M.J., Howard, R.A., Michels, D.J.: 1998, *Solar Phys.* **180**, 247

Koutchmy, S., Livshits, M.A.: 1992, *Space Sci. Rev.* **61**, 393

Kuiper, G.P.: 1953, *The Sun*, The University of Chicago Press, Illinois

Ludendorff, H.: 1928, *Sitzber. Preuss. Akad. Wiss.* **16**, 185

Mitchell, S.A.: 1929, *Handb. Aph.* **4**, 231

Saito, T., Akasofu, S.-I., Kozuka, Y., Takahashi, T., Numazawa, S.: 1993, *J. Geophys. Res.* **98**, 5639

Sýkora, J. Badalyan, O.G.: 1992, in *Proc. First SOHO Workshop*, ed.: ESA SP-348, 137, Sýkora, J., Ambrož, P.: 1995, in *24th International Cosmic Ray Conference* **4**, ed.: N. Iucci, Roma, 509

Sýkora, J., Ambrož, P.: 1997, in 'Theoretical and Observational Problems Related to Solar Eclipses', eds.: Z. Mouradian and M. Stavinschi, Kluwer Academic Publishers, Dordrecht, *NATO ASI Series C: Mathematical and Physical Sciences*, **494**, 111

Sýkora, J., Ambrož, P., Minarovjech, M., Obridko, V.N., Pintér, T., Rybanský, M.: 1998, *Solar Jets and Coronal Plumes*, ESA, **SP-421**, 79

Wilcox, J.M., Hundhausen, A.J.: 1983, *J. Geophys. Res.* **88**, 8095